Kinetics of the Reactions of Ethylene Oxide with Water and Ethylene Glycols

Georges A. Melhem,[a] Arturo Gianetto,[b] Marc E. Levin,[c] Harold G. Fisher,[d] Simon Chippett,[e] Surendra K. Singh,[a] and Peter I. Chipman[e]

[a] Arthur D. Little, Inc., Cambridge, MA 02140
[b] Dow Chemical Company, P.O. Box 8361, South Charleston, WV 25303
[c] Equilon Enterprises LLC, P.O. Box 1380, Houston, TX 77251
[d] Union Carbide Corporation, P.O. Box 8361, South Charleston, WV 25303
[e] Shell Chemical Company, P.O. Box 1380, Houston, TX 77251

This study of the water-contamination reactions of ethylene oxide was conducted by Arthur D. Little, Inc. with funding from, and under the auspices of, the Ethylene Oxide Industry Council, part of the American Chemistry Council. Significant experimental and technical contributions were also made by staff from Shell Chemicals' Westhollow Technology Center in Houston, Texas, and Union Carbide Corporation's Research Center in South Charleston, West Virginia. Unique fourth-order kinetics for the reactions of ethylene oxide with water, and ethylene oxide with ethylene glycols were derived and validated, as were kinetics for the reactions of neat ethylene oxide and the decomposition of ethylene glycols. The latter data was incorporated into a reaction model useful for the determination of ethylene oxide storage stability and pressure relief system design under water-contamination scenarios.

INTRODUCTION

The reactions of ethylene oxide with water, and ethylene oxide with ethylene glycols, to produce higher molecular weight glycols are widely practiced within the chemical process industries. Ethylene oxide must be stored and shipped to meet the demands for this versatile chemical. Contamination of this highly reactive chemical with almost any other substance should be avoided.

A number of incidents resulting from contamination with water have been reported:

A 22,500-gallon tank car containing 107,000 pounds of a 60:40 weight percent ethylene oxide-river water (pH ~ 6.8) mixture, with an estimated initial temperature of 12.5° C, was allowed to remain on a siding in the plant for approximately 23 days. A severe runaway reaction occurred, the safety relief valve malfunctioned, and the tank car ruptured due to overpressure. The time from first flow through the safety relief valve (75 psig set pressure) to rupture (estimated 1,200 psig) of the tank car was seven minutes [1].

A 24,000-gallon tank car containing 193,000 pounds of a 15:85 percent by weight ethylene oxide-brackish (Houston Ship Channel) river water mixture with a high salt content and assumed initial temperature of 27° C, ruptured after 14 hours. The tank car failed at a location where a mixed layer of ethylene oxide-water would have been in contact with the shell. The circumstances of loading water into the tank car for cleaning suggest that the water was layered below the pre-existing ethylene oxide in the tank car prior to the incident. Temperatures at the interface were high enough to cause the resulting incident [2].

This report presents, in detail, the kinetics, heats of reaction, stoichiometry, physical properties and vapor-liquid equilibria necessary to identify and mitigate hazardous water-contamination reactions of ethylene oxide and essentially neutral pH water. The information contained herein can also be used by knowledgeable persons to size pressure relief devices for inadvertent water contamination of vessels containing ethylene oxide.

ETHYLENE OXIDE REACTIONS

To successfully understand and model the behavior of mixtures of ethylene oxide and water, ranging from dilute to neat ethylene oxide, several chemical reactions should be considered:

1. Ethylene Oxide + Water → Ethylene Glycol
2. Ethylene Oxide + Ethylene Glycol → Diethylene Glycol (and higher glycols)
3. Ethylene Oxide → Acetaldehyde
4. Ethylene Oxide → Decomposition products
5. Ethylene Oxide → Ethylene Oxide Polymer
6. Ethylene Oxide Polymer → Decomposition products
7. Glycols → Decomposition products

Ethylene Oxide and Water Reactions (Neutral Medium)

Ethylene oxide reacts with water and ethylene glycols by addition polymerization to form higher ethylene glycols. As the water concentration increases, the onset (detection) temperature for the reaction in the Automatic Pressure Tracking Adiabatic Calorimeter (APTAC™) drops from approximately 200° C (neat ethylene oxide) to approximately 60° C at 25-38 weight percent water. The detected exothermic onset temperature then increases again as the concentration of ethylene oxide becomes too low to sustain a reaction of sufficient rate at lower temperature.

Monoethylene glycol is produced by reaction of ethylene oxide with water. Higher ethylene glycols are formed by the successive addition of ethylene oxide to glycol. Glycol product distributions are found to be well-represented by a Weibull-Nycander distribution [3]. In this model, a single activation energy describes the temperature dependence for all ethylene oxide addition reactions, but one rate is employed for characterizing monoethylene glycol formation, and a different rate coefficient is applied for forming all subsequent glycols. The ratio of the higher glycol rate coefficient to that for monoethylene glycol is defined as the Weibull-Nycander C-value. A C-value of two has been previously reported [3] and is confirmed in this study.

A Flory (Poisson) distribution predicts that the rate of each of these reactions are equal. A Natta distribution predicts that the rates of the successive reactions are different [3].

The heat of reaction of ethylene oxide with water is lower than the heats of reaction of ethylene oxide with mono and higher glycols. And, the neutral ethylene oxide reaction with water drifts toward an acidic pH and faster kinetics as the reaction proceeds [4]. The difference between unbuffered and buffered rate constants is only a few percent. Buffered solutions were not used during this study.

Ethylene Oxide and Water or Ethylene Glycol Reactions (Acidic Medium)

The rates of reaction of ethylene oxide with water, and ethylene oxide with ethylene glycols to produce higher molecular weight ethylene glycols by addition polymerization increase as the pH decreases, and are significantly faster in an acidic medium (pH 1-2) than rates in a neutral medium. The Weibull-Nycander model applies. Neutral glycol kinetics occur in parallel to the acid-catalyzed kinetics.

Ethylene Oxide and Water or Ethylene Glycol Reactions (Basic Medium)

The rates of reaction of ethylene oxide with water, and ethylene oxide with ethylene glycols to produce higher molecular weight ethylene glycols by additional polymerization, are significantly faster in a basic medium than in a neutral medium. The reaction rates, however, are slower than in an acidic medium. The Weibull-Nycander model again applies. Neutral glycol kinetics occur in parallel to the base-catalyzed kinetics.

Ethylene Oxide and Aqueous Sodium Hydroxide Reactions

Ethylene oxide reacts with the water introduced by contamination with aqueous sodium hydroxide to produce monoethylene glycol. This reaction is accelerated by the presence of sodium hydroxide. The sodium then associates with the glycols to produce sodium glycolates, and ethylene oxide reacts with the sodium glycolates to produce higher glycols. The rate of reaction of ethylene oxide with water to produce ethylene glycol is different from that of ethylene oxide with sodium glycolate to produce higher glycols (i.e., is consistent with the Weibull-Nycander model).

Two liquid phases (layers) can form when aqueous sodium hydroxide contaminates ethylene oxide. Kinetic data from the literature are typically mass-transfer limited. A triangular phase diagram, showing the soluble/insoluble regions, will be presented in a future report.

Polymerization

In the absence of contaminants, neat, commercial-grade, ethylene oxide was previously found to undergo a self-polymerization reaction starting at approximately 200° C in an Accelerating Rate Calorimeter (ARC®). A subsequent decomposition reaction follows [5].

HYDROLYSIS REACTION KINETICS

The kinetics for the reactions of ethylene oxide with neutral (5 < pH < 9) water, and ethylene oxide with ethylene glycols to produce higher glycols, have previously appeared in the open literature [4, 6, 7, 8]. Determining the reaction orders of these kinetics has been heavily influenced by the commercial concentrations of water (6-15 water-to-ethylene oxide mass ratio) used to maximize the production of ethylene glycol. Pseudo first-order kinetics will fit such conditions. Incorporating the typical water concentration into a first-order kinetic expression results in second-order kinetics, which also fit the experimental data.

Unimolecular Expressions

The literature [4, 6, 9, 10] provides rate expressions for reactions of ethylene oxide with water of the following type:

$$r_{EO} = -k_0[EO]\exp\left[-\frac{E}{RT}\right] \qquad (1)$$

where *[EO]* is the molar concentration of ethylene oxide in the mixture, k_0 is the frequency or preexponential factor, and E is the activation energy for the reaction. Note that this expression does not contain a term for concentration of any reactant other than ethylene oxide. This is adequate for solutions with low concentrations of ethylene oxide, where it is the limiting reactant, and is generally valid in commercial glycol reactors, where there is an excess of water. This expression will yield inaccurate results for solutions containing high concentrations of ethylene oxide.

Bimolecular Expressions

The following expression, proposed in the literature, is more useful for solutions containing high concentrations of ethylene oxide.

$$r_{EO} = A_0[EO][H_2O]\exp\left[-\frac{E}{RT}\right] \quad (2)$$

Most of the experimental data in the literature appear to be from solutions with low ethylene oxide concentrations. Expressions for base- and acid-catalyzed reactions are typically given in the form:

$$r_{EO} = A_0[EO][OH^-]\exp\left[-\frac{E}{RT}\right] \quad (3)$$

or,

$$r_{EO} = A_0[EO][H^+]\exp\left[-\frac{E}{RT}\right] \quad (4)$$

EXPERIMENTAL APPARATUS AND DATA ANALYSIS SOFTWARE

An extensive calorimetric and modeling study was conducted on the ethylene oxide-water reaction system. Experiments were carried out in the ARC and APTAC adiabatic calorimeters on mixtures of ethylene oxide-water, ethylene oxide-glycols, neat ethylene oxide and neat glycols. The experimental data were analyzed using SuperChems™, Version 4. In addition, independent analysis of the experimental data, as well as confirmation of the derived kinetic model, were conducted using other computer programs (e.g., SAFIRE).

Accelerating Rate Calorimeter (ARC)®

The accelerating rate calorimeter (ARC) is an instrument that can provide self-heat rate versus temperature-time data required for characterizing reactions. The adiabatic environment is accomplished by causing the temperature of the cell surroundings to match the temperature of the cell. The ARC can be used to obtain information on the thermal behavior of reactions and detected exothermic onset temperatures, primarily for liquid-phase reactive systems. It is also used for safety and/or performance evaluation of explosives and propellants. Self-heat rates at or above 0.02° C/min can be detected. This instrument (see Figure 1), described by Townsend and Tou [11], is known to provide thermokinetic data applicable to the design and safety performance evaluation of reactors and storage vessels. Such thermokinetic data include:

- rate of self-heating,
- adiabatic time to maximum rate,
- rate of pressure rise,
- maximum rate of reaction,
- kinetic parameters, (such as preexponential factor, activation energy, and reaction order) and
- heat of reaction.

The reaction mixture to be examined is introduced into a spherical cell with a volume of approximately 10 ml. The cell is equipped with a thermocouple mounted externally on the wall. Pressure is recorded by means of a transducer. Various cells, which have pressure ratings from 4,500 psi to 15,000 psi, can be used. As the pressure rating (that is, wall thickness for a cell) increases, the relative amount of heat absorbed by the cell itself, as indicated by the phi-factor, increases. The temperature and pressure of a test with a high phi-factor (specific heat of the sample plus the test cell divided by the specific heat of the test sample) must be corrected by established techniques to the low phi-factor conditions typical of many commercial operations. The high phi-factor can potentially mask exotherms that can occur at higher temperatures.

The significant advantage that the ARC offers over other calorimetric techniques is its high-sensitivity exothermic onset detectability of 0.02° C/min. The maximum self-heat rate is limited to approximately 10° C/min.

Automatic Pressure Tracking Adiabatic Calorimeter (APTAC)

The APTAC (see Figure 2) combines the features of the Design Institute For Emergency Relief Systems (DIERS) bench-scale apparatus (low phi-factor and high self-heat rates) and the ARC (low exotherm onset detection) into a single instrument.

The primary use of the APTAC is to obtain information on the thermal behavior and rates of reactions. Information obtained includes adiabatic temperature and pressure profiles for reactions. The basic data are manipulated to give self-heat and pressure rates as functions of temperature and time.

The reaction mixture to be examined is introduced into a spherical cell with a volume of approximately 130 ml. The cell is equipped with an internal thermocouple which directly measures the temperature of the reaction mixture. Four independent heaters with PID cascaded control maintain adiabatic conditions. Pressure is measured by means of a transducer. The cell is placed in a four-liter, high-pressure containment vessel rated to 2,500 psig. Non-isobaric pressure tracking by means of flow control valves prevents the cell from rupturing. Temperature and pressure rates of up to 400° C/min and 10,000 psi/min can be tracked. The

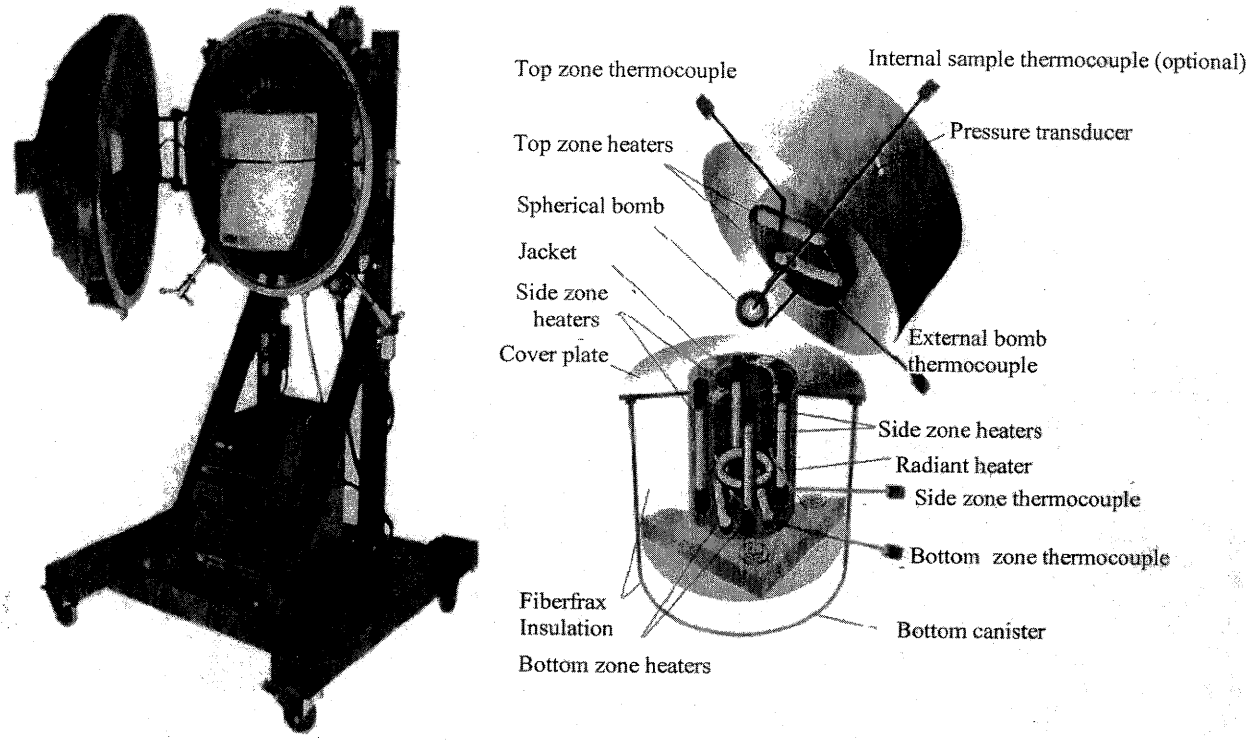

Figure 1. The accelerating rate calorimeter (ARC®).

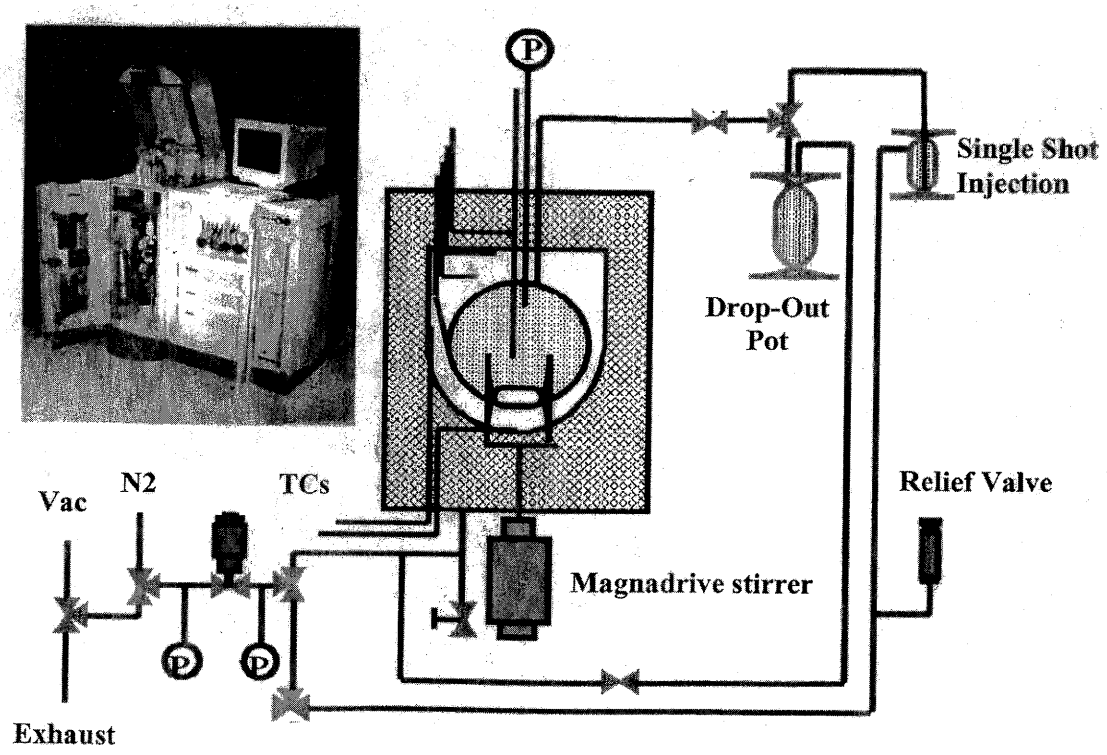

Figure 2. Automatic pressure tracking adiabatic calorimeter (APTAC™).

APTAC is a low phi-factor instrument (less than 1.15) with exotherm detection capabilities of 0.04° C/min [12].

SuperChems Computer Program

SuperChems [13, 14, 15] is an advanced tool for thermal hazards assessment, pressure relief design, and consequence analysis. The DIERS Edition is tailored to perform dynamic simulations of runaway chemical reactions, and design emergency relief systems for two-phase, vapor-liquid flows.

EXPERIMENTAL DATA SUMMARY

The experimental calorimetry data are summarized in Tables 1, 2, 3 and 4. Calorimetry data were collected in the ARC and APTAC on four systems:

1. Ethylene oxide and water
2. Ethylene oxide and glycols (mono and di)
3. Neat ethylene oxide
4. Neat glycols

The ethylene oxide-water tests (see Table 1) were collected over a wide range of phi-factors and ethylene oxide weight fractions (19 to 99 weight %). Representative self-heat rated data from selected tests are shown in Figure 3. These tests were conducted using a wide range of test cell materials of construction including titanium, Hastelloy-C, and glass. Detected onset temperatures measured in glass were higher than those measured in titanium or Hastelloy-C, especially for concentrated solutions of ethylene oxide and water/glycol. This can be attributed to possible reactivity at the cell wall or thermal inertia effects.

Although detected exothermic onset temperatures are useful in assessing the susceptibility of a system to a runaway reaction, experimental data must be used with an appreciation of the limits of the measuring instrument. Adiabatic calorimeters employed for assessing thermal stability can introduce adiabaticity, sensitivity, and thermal inertia effects.

Adiabaticity is defined as the fraction of the reaction energy being retained in a sample versus the cell at any instant. An adiabatic environment is one in which the reaction heat is neither lost from, nor energy gained by, a sample bomb in a laboratory apparatus. Adiabaticity is therefore a measure of heat losses to the environment.

Sensitivity is the ability of a laboratory instrument to measure (detect) the thermal parameters (onset temperature, etc.) of a runaway chemical reaction. For example, the ARC has a detection limit for measuring onset temperature corresponding to 0.02° C/min or 29° C/day. Obviously, the measured onset temperature would be much too high to directly use in making safety determinations. The measured data and the principles of thermal explosion theory should be used to make the temperature extrapolations required for safety-related decisions.

Thermal inertia is the ratio of the total heat of reaction to the heat absorbed by the sample in a laboratory instrument. The metal bomb of a laboratory apparatus is a significant heat sink. Thermal inertia is therefore the thermal capacity of the system (sample plus sample bomb) divided by the thermal capacity of the sample alone. Thermal inertia has the effect of dampening the magnitude of an observed runaway reaction. When the thermal inertia of the laboratory instrument is higher than the plant-scale equipment, the measured onset temperature can be too high, the rate of reaction too slow, the adiabatic temperature rise too low, and the pressure rise too low compared to what would be observed in a plant-scale environment. Again, the measured data and the principles of thermal explosion theory should be used to make the parameter extrapolations required for safety-related studies.

Accordingly, experimental results cannot be used directly as a measure of the appearance of reactivity, the time-to-maximum rate, the rate of reaction, the adiabatic temperature rise, or the maximum self-heat rate in commercial-scale equipment. Consult qualified personnel for interpretation of the data and guidance in the analysis of thermal stability or runaway reaction behavior in process vessels.

Figure 4 illustrates the impact of ethylene oxide weight fraction on the detected exothermic onset temperatures. The detected onset temperature goes through a minimum around 33%, and tends towards the value measured for neat ethylene oxide at 100%.

Of all of the compositions tested, the 25-38 weight % compositions have the lowest detected exothermic onset temperatures. Ethylene oxide-water solutions in this composition range have sufficient energy to reach the glycol decomposition temperature range of approximately 300° C. The glycol decomposition reactions are discussed elsewhere in this report and merit special consideration because they are very energetic and produce large amounts of gas.

The ethylene oxide and glycols tests (see Table 2) were conducted mostly in titanium test cells. The ethylene oxide composition ranged from 16 to 61 weight percent. The primary objective of conducting the ethylene oxide-glycols tests was to extract specific rate data on the ethylene oxide-glycol reaction. Once this was established, the impact of the reaction of ethylene oxide with water was easily quantified.

VAPOR-LIQUID EQUILIBRIUM

The ethylene oxide-water system is a highly non-ideal vapor-liquid equilibrium system. In order to properly interpret the experimental calorimetry data, by simulating the actual tests and scaling up the data, the mixture PVT behavior must be well-represented. The vapor-liquid equilibrium data for all of the binary systems of interest were obtained as follows:

1. Collect published literature data on all the systems.
2. Experimentally measure the vapor pressure data of pure glycols in the APTAC.
3. Perform VLE thermodynamic consistency checks using the Gibbs-Duhem relation.
4. Fit the binary interaction parameters using SuperChems Expert with the Melhem modification of the Peng-Robinson equation-of-state [16].

Experimental measurements of the vapor pressure curves for the pure glycols at low temperatures are necessary because they decompose at elevated temperature. The choice of critical properties is important

Table 1. APTAC™ Experimental calorimetry data summary for the ethylene oxide-water system.

Test Number	$T_{0,\Phi=1}$ (°C)	$T_{max,\Phi=1}$ (°C)	Φ	X_{EO} (wt %)	M_{total} (g)	Test Cell Material
A00245		108		10.12	60.09	TITANIUM
A00182	47.12	150	1.09	18.86	59.29	TITANIUM
A00118	56.97	209	1.09	32.00	59.03	TITANIUM
CMA12228	53.04	210	1.09	33.33	57.93	TITANIUM
RNWY2103	58.28	204	1.13	33.33	60.00	HASTELLOY-C
CMA04229	60.16	246	1.22	50.02	48.42	GLASS
A00124	69.73	260	1.20	58.28	32.86	TITANIUM
A00123	70.71	236	1.20	58.31	32.62	TITANIUM
CMA05129	70.86	341	1.28	60.14	41.82	GLASS
A00170	82.64	236	1.28	74.48	25.35	TITANIUM
A00168	62.98	NA	1.29	74.71	25.58	TITANIUM
CMA05139	92.46	NA	1.48	74.99	27.43	GLASS
A00173	112.09	NA	1.64	89.75	20.49	GLASS
A00171	119.65	NA	1.39	89.83	21.24	TITANIUM
CMA05109	138.79	NA	1.64	91.22	23.36	GLASS
A00113	282.74	NA	1.45	97.97	19.70	TITANIUM
A00114	271.67	NA	1.47	98.93	18.71	TITANIUM

Φ = Thermal inertia
T_0 = Detected onset temperature at 0.06°C/min; corrected to Φ of 1
T_{max} = Measured maximum reaction temperature; NOT corrected for thermal inertia
M_{total} = Total sample mass of ethylene oxide and water
All tests were stirred

Table 2. APTAC™ Experimental calorimetry data summary for the ethylene oxide-glycols systems.

Test Number	$T_{0,\Phi=1}$ (°C)	Φ	X_{EO} wt %	M_{EO} (g)	M_{EG} (g)	M_{DEG} (g)	M_{H2O} (g)	M_{Total} (g)	Test Cell Material
RNWY2421	66.77	1.12	18.41	12.07	53.50			65.57	TITANIUM
A00180	44.49	1.14	21.93	12.47	44.38			56.85	TITANIUM
A00139A	64.20	1.14	23.66	13.99	45.13			59.12	TITANIUM
RNWY2420	73.57	1.14	25.00	15.00	45.00			60.00	TITANIUM
CMA01139	58.03	1.14	25.02	15.02	45.00			60.02	TITANIUM
RNWY2418	70.03	1.14	25.26	15.11	44.70			59.81	TITANIUM
RNWY2419	76.79	1.13	26.78	16.62	45.43			62.05	TITANIUM
CMA04239B	62.37	1.27	33.47	16.00	31.80			47.80	GLASS
A00181	58.39	1.16	35.47	18.40	33.47			51.87	TITANIUM
A00134A	76.22	1.15	46.35	26.67	30.87			57.54	TITANIUM
A00136A	75.35	1.14	48.96	29.77	31.03			60.80	TITANIUM
CMA01089	60.05	1.20	51.22	21.05	20.05			41.10	TITANIUM
CMA12248	67.76	1.13	50.00	30.85	30.85			61.70	TITANIUM
CMA01119	64.05	1.30	50.00	14.10	14.10			28.20	TITANIUM
RNWY2412	85.74	1.15	52.59	30.48	27.48			57.96	TITANIUM
A00183	83.95	1.29	60.66	18.47	11.98			30.45	TITANIUM
A00200	85.18	1.14	16.63	10.61		53.20		63.81	TITANIUM
A00195	92.23	1.15	32.21	18.05		37.99		56.04	TITANIUM
A00194	53.61	1.19	32.16	12.23	20.01		5.79	38.03	TITANIUM

Φ = Thermal inertia
T_0 = Detected onset temperature at 0.04°C/min; corrected to Φ of 1
M_{Total} = Total sample mass
All tests were stirred

Table 3. Experimental calorimetry data summary for neat ethylene oxide.

Test Number	Test Type	$T_{0,\Phi=1}$ (°C)	Φ	M_{EO} (g)	Test Cell Material
C02269	ARC®	237	5.47	3.61	HASTELLOY-C
C03309	ARC®	254	8.14	3.26	HASTELLOY-C
A03269	ARC®	234	4.83	6.06	HASTELLOY-C
C04029	ARC®	223	5.93	4.73	HASTELLOY-C
CM04219A	APTAC™	210	1.46	30.00	GLASS
A00105	APTAC™	210	1.29	32.00	TITANIUM
A00106	APTAC™	258	1.44	20.00	TITANIUM
A00107	APTAC™	240	1.47	20.00	TITANIUM
A00109	APTAC™	253	1.44	20.00	TITANIUM
A00110A	APTAC™	247	1.47	19.37	TITANIUM
A00111A	APTAC™	266	1.47	19.69	TITANIUM

Φ = Thermal inertia
T_0 = Detected onset temperature at 0.02°C/min (ARC®) or 0.04°C/min (APTAC™)
All APTAC™ tests were stirred; all ARC® tests were unstirred

Table 4. Experimental calorimetry data summary for neat glycols.

Test Number	Test Type	$T_{0,\Phi=1}$ (°C)	T_P (°C)	Φ	Glycol Type	M_{Total} (g)	Test Cell Material
CMA08119B	APTAC™	314	333	1.20	Mono	40.04	TITANIUM
CMA08119A	APTAC™	340	303	1.21	Di	40.01	TITANIUM
81899	APTAC™	365	329	1.21	Di	40.00	TITANIUM
CMA08129	APTAC™	341	312	1.20	Tri	40.08	TITANIUM
CMA08159	APTAC™	340	328	1.20	Tetra	40.94	TITANIUM
B042901	ARC®	330	304	1.54	Mono	4.02	TITANIUM
C08169	ARC®	350	275	1.56	Di	4.00	TITANIUM
C08179	ARC®	340	306	1.54	Tri	4.00	TITANIUM
C08189	ARC®	340	312	1.54	Tetra	4.00	TITANIUM

Φ = Thermal inertia
T_0 = Detected onset temperature at 0.02°C/min (ARC®) or 0.04°C/min (APTAC™)
T_P = Detected onset temperature at dP/dt = 0.1 psi/min
All APTAC™ tests were stirred and conducted at 10°C increments
All ARC® tests were unstirred

for experimental data interpretation of the ethylene oxide-water-glycol reacting mixture phase behaviors.

To illustrate the highly non-ideal phase behavior of the system, Figures 5 and 6 show a comparison between experimental VLE data at 1.013 bars for ethylene oxide-water, and model predictions of the data using ideal behavior and the Peng-Robinson equation-of-state. An ideal phase behavior assumption will lead to the wrong prediction of the vapor-liquid split in the vessel, and, as a result, to an erroneous energy balance and temperature/pressure behavior. This, in turn, can lead to incorrect prediction of relief system activation.

Literature references for various component pair vapor-liquid equilibria data are provided in Table 5.

The binary interaction parameters used in the final simulations are as follows:

Ethylene oxide-water	k_{ij} = -0.1044,	λ_{ij} = -0.0895
Ethylene glycol-water	k_{ij} = -0.0383,	λ_{ij} = 0.
Diethylene glycol-water	k_{ij} = -0.107,	λ_{ij} = 0.
Triethylene glycol-water	k_{ij} = -0.134,	λ_{ij} = 0.
Ethylene oxide-ethylene glycol	k_{ij} = 0.,	λ_{ij} = 0.
Ethylene oxide-diethylene glycol	k_{ij} = 0.0196,	λ_{ij} = 0.

ETHYLENE OXIDE HYDROLYSIS REACTION MODEL

The data presented herein are believed to cover the widest range of concentrations and reaction temperatures available in the open literature. The published kinetic models presented under Experimental Apparatus and Data Analysis Software, however, do not adequately fit our entire data set (see Figure 4). In papers

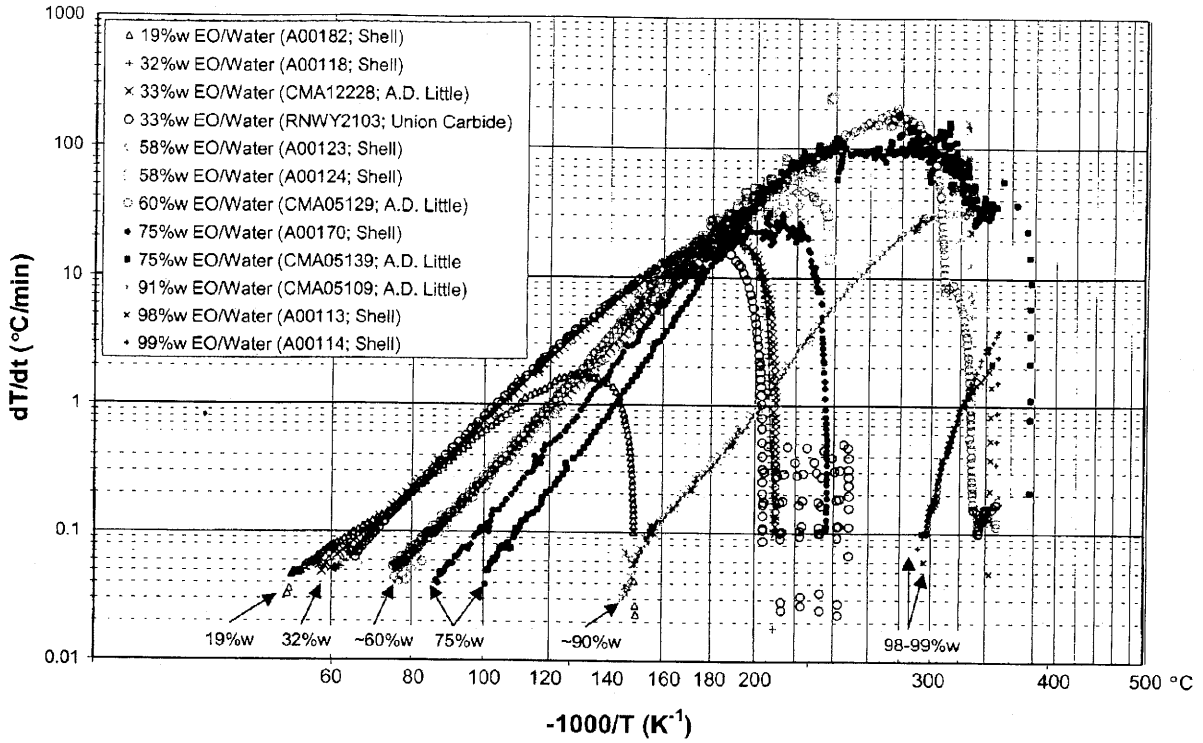

Figure 3. Self-heat rate data for selected ethylene oxide-water APTAC™ tests.

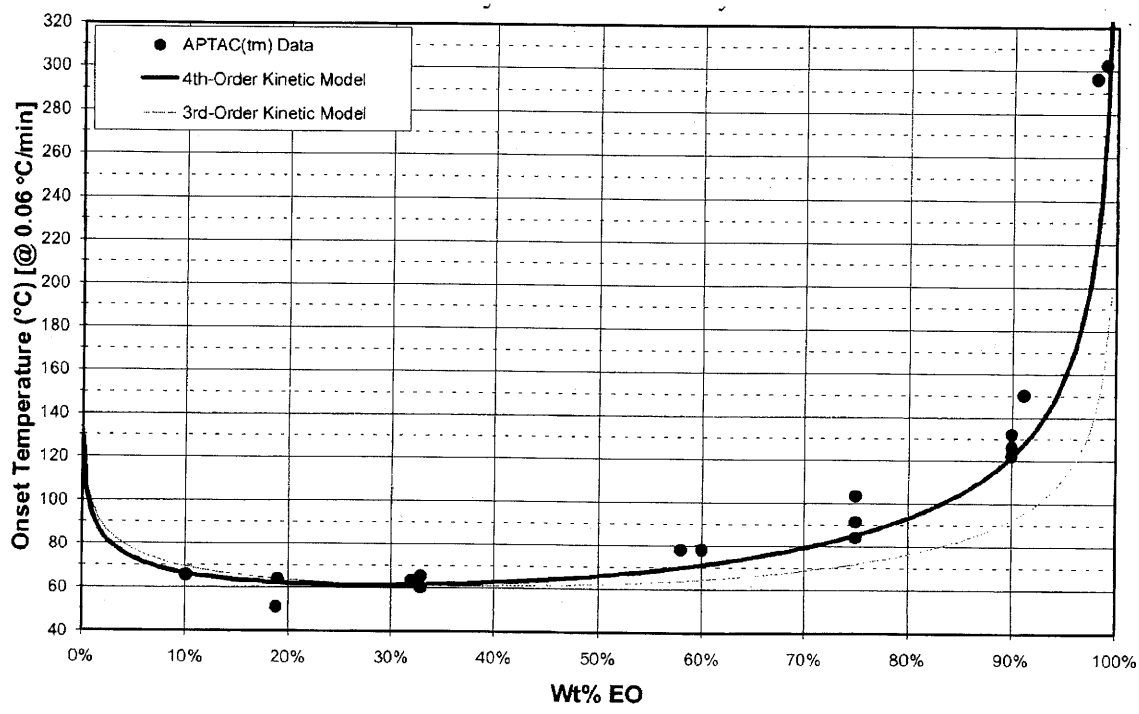

Figure 4. A comparison of measured and predicted onset temperatures (for a specified self-heat rate) as a function of reaction order for the ethylene oxide-water system.

by Virtanen [7, 34], reaction kinetics with higher order water dependencies were developed on mechanistic arguments and fit to experimental data. We have chosen to explore higher order reaction models that bear some similarities to Virtanen's (such as an overall fourth-order model dependence), but which also contain some key distinguishing features. The acid- and base-catalyzed reactions of ethylene oxide and water to produce ethylene glycols will be covered in separate proposed papers.

These kinetics were fit by the following simulation procedure:

Table 5. Literature sources for thermodynamic component pair data.

	Water	EO	EG	DEG	TEG	T4EG	P5EG
Water							
EO	17-20,*						
EG	21-28	*					
DEG	22,24,26,*	*	26				
TEG	24,29	---	---	26			
T4EG	29,30	---	---	---	---		
P5EG	31-33	---	---	---	---	---	

*Includes internal corporate data.

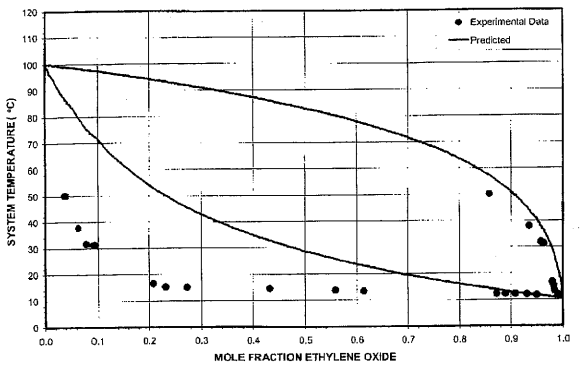

Figure 5. Comparison of experimental TXY data and ideal behavior predictions for the ethylene oxide-water system at 1.013 bars (see Table 5).

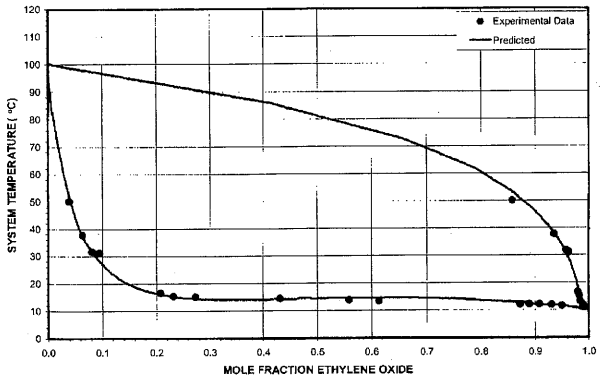

Figure 6. Comparison of experimental TXY data and Peng-Robinson equation of state predictions for the ethylene oxide-water system at 1.013 bars (see Table 5).

1. Select reaction orders and activation energies as starting estimates.
2. Simulate the ARC/APTAC tests, including the heat-wait-search steps [15].
3. Compare the model predictions of temperature rise rate-temperature, pressure rise rate-temperature, pressure-temperature, temperature-time, and pressure-time to experimentally-measured values.
4. If the model predictions do not agree with the measured values, go back to step 1; otherwise stop.

Particular emphasis was placed on the ability of the model to predict the detected onset temperature at both low and high concentrations of ethylene oxide. Reaction orders of one, two and three were examined as candidates. These models performed reasonably well in the low concentration range, but underpredict the detected onset temperatures at high ethylene oxide concentrations. The overall fourth-order reaction rate expression was found to accurately predict the reaction kinetics of ethylene oxide with neutral water (between 10 and 90 wt % EO), ethylene oxide with ethylene glycol (between 18 and 61 wt % EO), and some exploratory runs with diethylene glycol.

Kinetics

Hydrolysis Reaction

Ethylene oxide reacts with water in the liquid phase to produce monoethylene glycol according to the following stoichiometry:

$$C_2H_4O + H_2O \rightarrow C_2H_6O_2 \quad (5)$$

or

(6)

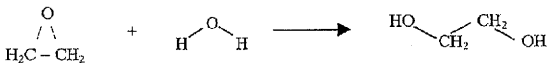

The rate of reaction is given by the following expression:

$$r_1 = k\,[EO]\,[H_2O]\,[ROH]^2 \quad (7)$$

where r_i is in kmol/m^3/s, and k is an Arrhenius factor defined as:

$$k = A\exp\left[-\frac{E}{RT}\right] \quad (8)$$

where A and E have been determined to be:

$$A = 338\ (m^3)^3 kmol^{-3} s^{-1} \quad (9)$$

$$\frac{E}{R} = 9525 \text{ Kelvins or } E = 18880 \text{ cal / gmol} \quad (10)$$

and $[ROH]$ is given by:

$$[ROH] = [H_2O] + 2[EG] + 2[DEG] + 2[TEG] + 2[T4EG] + 2[P5EG] + \text{etc.} \quad (11)$$

The value of the preexponential factor A has an uncertainty of ±10%. Note that the $[ROH]$ term accounts for the total molar concentration of independent hydroxyl groups in solution. The units in the above expressions are in SI, i.e., m, kmol, s, etc. It is important to emphasize that in Virtanen's mechanistic development [7], only water was considered to associate with ethylene oxide. Our own modeling is more accurate because it considers all species containing hydroxyl groups. Moreover, the current study also takes into account the impact of the subsequent reactions of the ethylene glycols on the overall kinetics results.

Glycol Reaction

Ethylene oxide reacts with glycols to make higher-order glycols and polyglycols. The reactions of ethylene oxides with glycols occur based on the following stoichiometry:

$$C_2H_4O + C_{2i-2}H_{4i-2}O_i \rightarrow C_{2i}H_{4i+2}O_{i+1},\ i = 2,\ldots,\ 6 \quad (12)$$

The reactions between ethylene oxide and the glycols proceed according to the following expression:

$$r_2 = 2k\,[EO]\,[C_{2i-2}H_{4i-2}O_i]\,[ROH]^2,\ i = 2,\ldots,\ 6 \quad (13)$$

where k and $[ROH]$ are defined earlier.

Mechanistic Justification

These kinetics are consistent with the following two reactions occurring in sequence:

1. Ethylene oxide is assumed to rapidly associate with two moles of hydroxyl to form an intermediate, I

$$EO + 2ROH \Leftrightarrow I \quad (14)$$

The concentration of ROH is defined in Equation 11. The glycol concentration terms in Equation 11 are multiplied by two to account for the presence of two hydroxyl groups on each glycol molecule.

This reaction is presumed to be so fast that chemical equilibrium is attained. Hence:

$$K = \frac{[I]}{[EO][ROH]^2} \quad (15)$$

where K is the equilibrium constant for this reaction.

2. This intermediate is presumed to react slowly with water to form EG, with EG to form DEG, with DEG to form TEG, etc., regenerating the two moles of ROH.

$$I + H_2O \rightarrow EG + 2ROH \quad (16)$$

$$r_{EG} = k_0\,[I]\,[H_2O] \quad (17)$$

where the subscript EG implies the formation rate from H_2O and does not evaluate the consumption of EG in subsequent reactions. If EG is being converted to DEG, the following reaction and reaction rate apply:

$$I + EG \rightarrow DEG + 2ROH \quad (18)$$

$$r_{DEG} = 2k_0\,[I]\,[EG] \quad (19)$$

The factor of two applies because either of the two hydroxyls on the ethylene glycol can undergo reaction. Equations 18 and 19 apply in the exact same manner for all the heavier glycols. The intermediate concentration $[I]$ has not been measured in this study, but can be expressed per Equation 15 as:

$$[I] = K[EO]\,[ROH]^2 \quad (20)$$

This expression for $[I]$ can be substituted into Equations 16 and 19, which yields for the reactions described herein:

$$r_{EG} = k_0\,K[EO]\,[H_2O]\,[ROH]^2 \quad (21)$$

$$r_{DEG} = 2k_0\,K[EO]\,[EG]\,[ROH]^2 \quad (22)$$

It is convenient to combine k_0, K as k:

$$k = k_0K \quad (23)$$

The final rate expression is given by the following equations:

$$r_{EG} = k[EO]\,[H_2O]\,[ROH]^2 \quad (24)$$

$$r_{DEG} = 2k[EO]\,[EG]\,[ROH]^2 \quad (25)$$

Model Comparisons

The aggregate dependence on species concentrations is fourth order. The same energy of activation and the same preexponential factor were found to predict adequately the onset temperature and heat rate for both the hydrolysis reaction of ethylene oxide with water, and the ethoxylation reaction of ethylene oxide with glycols. A single fourth-order reaction model accurately predicts the experimental results.

Consideration was also given to a third-order reaction model. A third-order reaction mechanism implies that only one hydroxyl group associates with ethylene oxide to form the intermediate vs. two hydroxyl groups in the fourth-order reaction mechanism.

A comparison of predicted onset temperatures (0.06° C/min heat rate) for a third-order reaction and a fourth-order reaction versus weight percent ethylene oxide is shown in Figure 4. The experimental detected onset temperatures (unadjusted for thermal inertia)

Table 6. Measured heats of reaction from calorimetry data.

Chemical Name		Mw	Heat of Reaction (liquid phase) (kJ/kg EO)	Heat of Reaction (liquid phase) (BTU/lb EO)
Ethylene oxide	(EO)	44.053		
Water	(H_2O)	18.016		
Ethylene glycol	(EG)	62.068	-2,064	-887
Diethylene glycol	(DEG)	106.122	-2,205	-948
Triethylene glycol	(TEG)	150.175	-2,375	-1,021
Tetraethylene glycol	(T4EG)	194.228	-2,410	-1,036
Pentaethylene glycol	(P5EG)	238.280	-2,424	-1,042
Hexaethylene glycol	(HEG)	282.330	-2,424	-1,042
Polyethylene glycol		326	-2,489	-1,070

ΔH_f is the heat of formation at 25°C
Subscript l indicates liquid phase
Subscript g indicates gas phase
λ is the latent heat of vaporization at 25°C

Table 7. Comparison of calculated formation energies from APTAC™ data with reported literature values.

Chemical Name	Phase	$-\Delta H_f$ (kJ/kg)	Accuracy (+/-) (kJ/kg)	Source
Ethylene glycol	Gas	6,251	32.22	NIST Review
	Gas	6,354	45.11	NIST Review
	Gas	6,272	Unknown	DIPPR
	Gas	6,172		This work
	Liquid	7,301	19.50	NIST Review
	Liquid	7,411	45.11	NIST Review
	Liquid	7,322		This work
Diethylene glycol	Gas	5,382	161.46	DIPPR
	Gas	5,256		This work
	Liquid	5,923	22.42	NIST Review
	Liquid	5,931		This work
Triethylene glycol	Gas	4,828	144.84	DIPPR
	Gas	4,710		This work
	Liquid	5,406		This work
Tetraethylene glycol	Gas	4,543	Predicted	DIPPR
	Gas	4,486		This work
	Liquid	5,055	23.68	NIST Review
	Liquid	5,127		This work

were added to the plot in order to show that the fourth-order reaction mechanism predicts the data more accurately, particularly at high ethylene oxide concentration. At 10 to 40 wt % ethylene oxide concentration the rates of reaction for a third-order reaction and fourth-order reaction are very similar. However, a divergence occurs once the concentration of ethylene oxide is greater that 40 wt %.

A parity plot appears in Figure 7, consisting of individual points from the observed self-heat rate data between onset temperature and up to 200° C (or the peak heat rate) as compared to the self-heat rates calculated from the model. Excellent agreement is seen between the rates measured and those predicted from the proposed kinetic model.

Heat of Reaction Data

The present model terminates to an oligomer with a molecular weight of 326 (see Table 6). The complete series of ethylene oxide addition reactions are defined

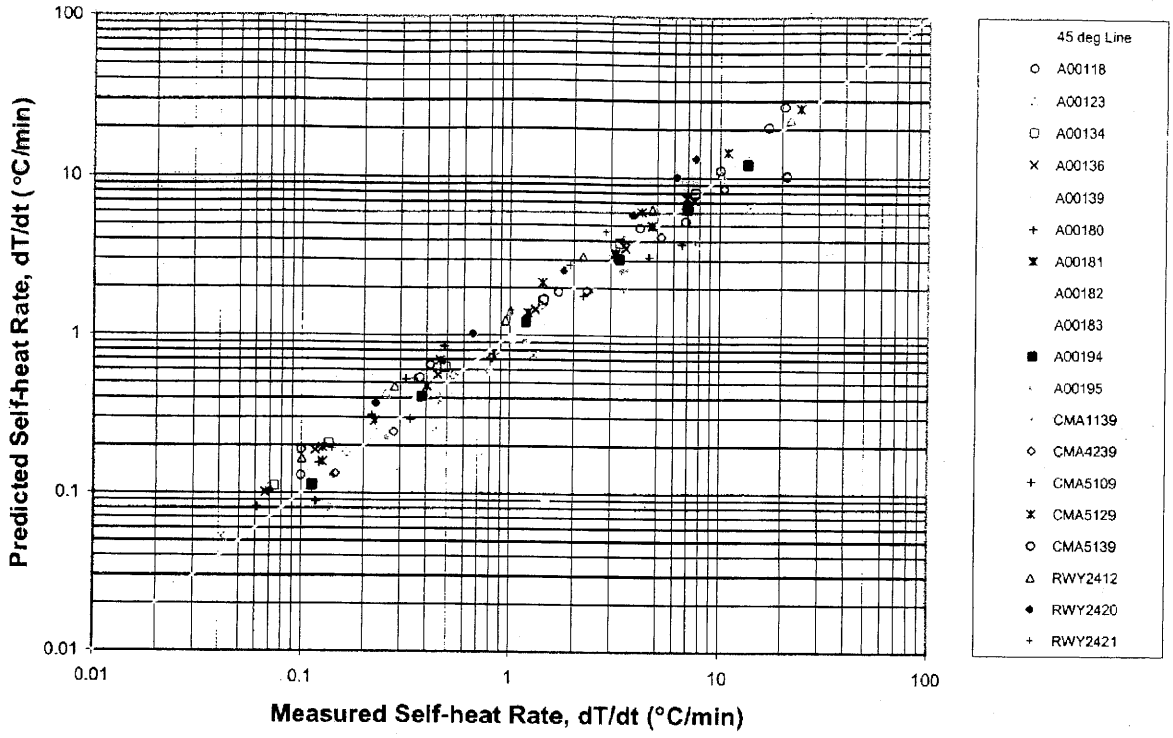

Figure 7. Parity plot of self-heat rates measured in the APTAC™ vs. self-heat rates predicted from the kinetic model.

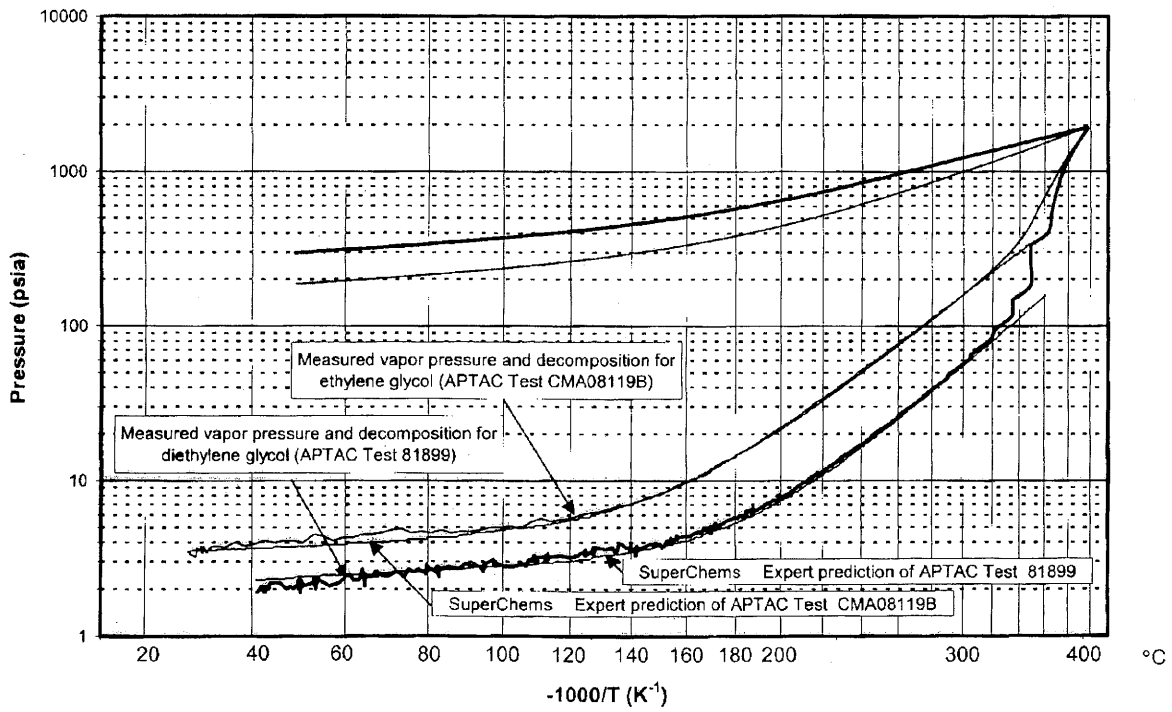

Figure 8. Measured vs. predicted vapor pressure data for ethylene glycol and diethylene glycol.

Table 8. Gas chromatograph characteristics.

Instrument	Lab 1	Lab 2
Instrument	HP 5890	HP 5890
Injector	Split (200:1 ratio)	
Injector Temperature (°C)	250	250
Column Type	J&W bonded phase DB-1 fused-silica	RTX 5-Amine
Column Length (m)	30	30
Column Diameter (mm)	0.32	0.32
Column film Thickness (mm)	1.0	1.0
Carrier Gas	Helium	Helium
Carrier Gas Flow Rate (ml/min)	30	35
Pressure Ramp		No
Initial Temperature (°C)	100	35
Ramp Rate (°C/min)	10	15
Final Temperature (°C)	260	220
Retention Times (min)		
EG	2.0	6.7
DEG	4.3	11.3
TEG	8-9	14.9
T4EG	12.6	18.8
Detector	FID	FID
Detector Temperature (°C)	300	300

Table 9. Measured vs. predicted product distribution analysis for selected tests.

Weight Fraction (%)	Test Number				
	A00123	A00180	A00182	RNWY2421	RNWY2418
Starting composition					
Ethylene oxide	58.31	21.93	18.86	18.41	25.56
Water	41.69	0.00	81.14	0.00	0.00
Ethylene glycol	0.00	78.07	0.00	81.59	74.44
Ending composition	Meas / Pred	Meas / Pred	Meas / Pred	Meas / Pred	Meas / Pred
Water	28.1 / 28.2	1.63 / 0.00	73.0 / 73.9	NA / 0.00	NA / NA
Ethylene glycol	34.9 / 31.0	49.1 / 50.5	18.6 / 22.3	62.0 / 59.4	46.0 /46.9
Diethylene glycol	24.7 / 24.7	31.5 / 36.3	3.20 / 3.40	30.2 / 32.2	33.6 / 37.6
Triethylene glycol	10.0 / 11.6	9.2 / 10.8	<4 / 0.3	6.00 / 7.20	15.6 / 12.5
Tetraethylene glycol	2.90 / 3.70	<4 / 2.00	NA / 0.02	0.30 / 0.90	1.96 / 2.50
Pentaethylene glycol	NA / 0.90	NA / 0.90	NA / 0.00	NA / 0.10	2.00 / 0.37

earlier by Equations 5 and 12. The experimental calorimetry data collected in this study yield the heats of reaction for the individual steps summarized in Tables 6 and 7.

As reflected in the parity plot of Figure 7, the predicted onset temperatures (for a given self-heat rate), slopes of the heat rate curve, and peak heat rates match the experimental data for all concentrations of ethylene oxide with water. This was also found to be the case for the EO-EG experiments. However, the adiabatic temperature rise was difficult to predict, in some cases. A possible explanation for these discrepancies is that an additional reaction is occurring in the system, such as ethylene oxide polymerization or isomerization.

Product Distribution Predictions

A compositional analysis of the liquid reaction product distribution was conducted at the end of selected tests to provide more insight into the reaction stoichiometry. The measured product distribution data also serves as experimental verification of the proposed reaction model.

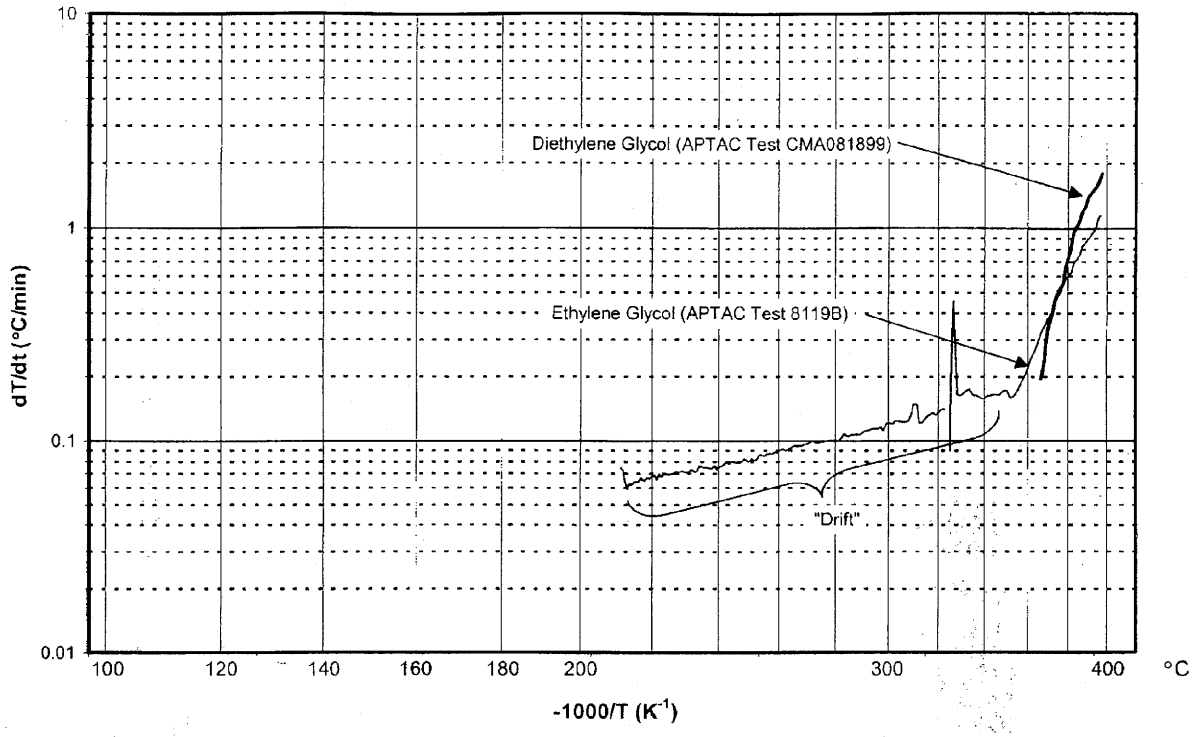

Figure 9. Measured and decomposition onset temperatures for ethylene glycol and diethylene glycol.

The product distribution analysis was conducted on a HP 5890 gas chromatograph equipped with a split injection system. The approximate retention times (min) for ethylene glycol, diethylene glycol, triethylene glycol and tetraethylene glycol are shown in Table 8.

The results indicate that the reaction model is robust because the predictions were very close to actual measurements. Table 9 summarizes the product analysis predictions vs. measured values for the selected tests.

NEAT ETHYLENE OXIDE REACTIONS

Neat ethylene oxide can decompose in both the liquid and vapor phase. These decompositions occur at high temperatures and are heavily influenced by the presence of contaminants, such as rust, for example. The vapor pressure of neat ethylene oxide at decomposition temperatures is extremely high. Most emergency relief systems dealing with neat ethylene oxide would relieve before decomposition temperatures are reached. It is important to note that large amounts of ethylene oxide should not be discharged to the open atmosphere as this can lead to a vapor cloud deflagration, as well as a toxicity hazard.

GLYCOLS DECOMPOSITION

Table 4 summarizes the data collected in the ARC and APTAC on neat glycols. The purpose of these measurements was to validate the SuperChems model predictions of the glycols' vapor pressures, and to measure the onset temperatures for the decomposition of the neat glycols.

Figure 8 compares the SuperChems model predictions of ethylene glycol and diethylene glycol vapor pressure data. Excellent agreement with the experimental data is obtained up to the decomposition point.

Neat glycols, when heated to approximately 300° C, decompose by exothermic, autocatalytic kinetics to volatiles and non-condensable gases. This is shown in Figure 9 and Table 4. Pressure increases, indicating the onset of decomposition, could be detected during ethylene oxide-water experiments accompanied by a high adiabatic temperature rise. Note that the presence of sodium hydroxide [35] or potassium hydroxide or strong acid, depending upon the concentration, reduces the detected decomposition onset temperature to approximately 175° to 200° C. Appropriate kinetics, stoichiometry, heats of reaction, vapor-liquid equilibria, and physical properties were employed to model the effects of the neat glycol decomposition reactions when determining kinetics for the high temperature, ethylene oxide hydrolysis reactions.

The glycol decomposition reaction model and experimental verification will be published in the literature in the coming months. The DIERS Users Group has also published Round-Robin test data and model parameters for the decomposition of the glycols [35].

SAFE HANDLING OF ETHYLENE OXIDE

The kinetics, heats of reaction, stoichiometry, physical properties, and vapor-liquid equilibria models presented in this report were incorporated into a digital simulation computer program, which was used to predict the first ethylene oxide-water contamination incident discussed in the Introduction section. The tank car was insulated. With an estimated initial contents temperature of 12.5° C, the tank car initially gained and then lost heat to the atmosphere as the

temperature of the reacting mixture increased. The simulation predicted a time to maximum rate of 21.8 days compared to the actual incident time of 23 days.

It is important to note that the estimated initial self-heat rate of the previously-mentioned 22,500-gallon tank car incident was 0.8° C per day. This is considerably lower than the calorimeter detection limit of 58° C/day (equal to 0.04° C/min) in the APTAC and illustrates the caution that must be exercised when inferring maximum operating temperatures from calorimeter data.

DESIGN OF EMERGENCY RELIEF SYSTEMS

A design scenario for relief sizing is developed by first defining the process conditions at the time of initiation of a proposed emergency event. Then, the course of the event is tracked either by calculations or logic exercises to the point of most-severe venting conditions or to the maximum allowable pressure level of the equipment. Other possible events are treated likewise in order to select the worst credible case for the design basis. The emergency relief device set pressure is put at or below the vessel maximum allowable working pressure, depending on the anticipated pressure history of the selected scenario. From this, a vent rate is determined, which will just prevent the pressure from rising above the maximum allowable venting pressure for the equipment. This is the "minimum required relief capacity." A standard-size relief device is selected to have at least this much flow. Alternate scenarios might have to be carried along to this point to identify worst case (largest relief). Recent AIChE/DIERS publications [36, 37] provide information useful for the design of emergency relief systems.

DESIGN OF EFFLUENT HANDLING SYSTEMS

The design scenario for effluent-handling systems can differ from that selected for relief sizing. For example, an emergency vapor-venting scenario can require a larger relief size than liquid or two-phase events. Nevertheless, provisions must be made for liquid handling if liquid or two-phase venting scenarios are credible. In the case of two-phase venting, the worst instant for handling a given phase may differ from the conditions at the worst instant for relief sizing. A time-history prediction of the event may not be required for relief sizing, but is often desirable for establishing the maximum design loads on the effluent system equipment. Venting simulation programs, such as SuperChems, provide such a history for proposed scenarios. A recent AIChE/DIERS publication [37] provides information useful for the design of effluent handling systems.

ACKNOWLEDGMENTS

This study was conducted by Arthur D. Little, Inc. with funding from, and under the auspices of, the American Chemistry Council Ethylene Oxide Industry Council. A subcommittee of the Safety Task Group, including P.I. Chipman (Chair–Shell Chemical Company), M.B. Lakin (Past Chair–Celanese, Ltd.), and R.A. Lenahan (ARCO/Lyondell), provided project oversight. Kathleen M. Roberts, Kathryn Smith, and Karyn Schmidt of the ACC staff provided contract administration.

TRADEMARKS

APTAC™ is a trademark of Arthur D. Little, Inc.
ARC® is a registered trademark of Arthur D. Little, Inc.
SuperChems™ is a trademark of Arthur D. Little, Inc.

LITERATURE CITED

1. **MacCutcheon, S.M.**, "Ethylene Oxide Explosion Freeport, Texas," Letter to members of the MCA Safety and Fire Protection Committee, March 11, 1974.
2. **Vanderwater, R.G.**, "Case History of an Ethylene (Oxide) Tank Car Explosion," *Chemical Engineering Progress*, 85, 12, pp 16–20, December 1989.
3. **Weibull, B. and B. Nycander**, "The Distribution of Compounds Formed in the Reaction Between Ethylene Oxide and Water, Ethanol, Ethylene Glycol, or Ethylene Glycol Monoethyl Ether," *Acta Chemica Scandinavica*, 8, 5, pp 847–858, 1954.
4. **Lichtenstein, H.J. and G.H. Twigg**, "The Hydration of Ethylene Oxide," *Trans. Faraday Soc.*, 44, pp 905–909, 1948.
5. **Britton, L.G.**, "Thermal Stability and Deflagration of Ethylene Oxide," *Plant/Operations Progress*, 9, 2, pp 75–86, April 1990.
6. **Koskikallio, J. and E. Whalley**, "Effects of Pressure on the Spontaneous and the Base-Catalyzed Hydrolyses of Epoxides," *Canadian J. Chem.*, 37, pp 783–787, 1959.
7. **Virtanen, P.O.I.**, "Kinetics of the Hydrolysis Reactions of Ethylene Oxide," *Ann. Academiae Scientiarum Fenricae*, A, pp 9–89, 1963.
8. **Virtanen, P.O.I.**, "The Vapour Pressure and Activity of Ethylene Oxide Dissolved in Various Water-Organic Solvent Mixtures, Kinetics of the Uncatalyzed Hydrolysis of Ethylene Oxide," *Suomen Kemistilehti*, B39, pp 115–122, 1966.
9. **Bronsted, J.N., M. Kilpatrick, and M. Kilpatrick**, "Kinetic Studies on Ethylene Oxides," *JACS*, 51, pp 428–461, 1929.
10. **Dever, J.P., K.F. George, W.C. Hoffman, and H. Soo**, "Ethylene Oxide," *Kirk-Othmer Encyclopedia of Chemical Technology, 4th Edition, Volume 9*, J.I. Kroschwitz, Editor, John Wiley & Sons, New York, NY, pp 915-959, 1994.
11. **Townsend, D.I. and J.C. Tou**, "Thermal Hazard Evaluation by an Accelerating Rate Calorimeter," *Thermochemica Acta*, 37, pp 1–30, 1980.
12. **Young, M.A. and S. Chippett**, "Design and Operation of an Automatic Pressure Tracking Adiabatic Calorimeter (APTAC™)," *International Symposium on Runaway Reactions and Pressure Relief Design*, G.A. Melhem and H.G. Fisher, Editors, pp 23–57, AIChE, DIERS, New York, NY, 1995.
13. **Melhem, G.A. and H.G. Fisher**, "An Overview of SuperChems™ for DIERS: A Program for Emergency Relief System and Effluent Handling Designs," *Process Safety Progress*, 16, 3, pp 185–197, Fall 1997.

14. **Melhem, G.A.**, "Advanced ERS Design Using Computer Simulation," *International Symposium on Runaway Reactions and Pressure Relief Design*, G.A. Melhem and H.G. Fisher, Editors, pp 502–566, AIChE, DIERS, New York, NY, 1995.
15. **Melhem, G.A., H.G. Fisher, and D.A. Shaw**, "An Advanced Method for the Estimation of Reaction Kinetics, Scale-up and Pressure Relief Design," *Process Safety Progress*, 14, 1, pp 1–21, January 1995.
16. **Melhem, G.A., R. Saini, and B.M. Goodwin**, "A Modified Peng-Robinson Equation of State," *Fluid Phase Equilibria*, 47, pp 189–237, 1989.
17. **Coles, K.F. and F. Popper,** *Ind. Eng. Chem.*, 42, pp 1434-1438, 1950.
18. **MacCormack, K.E. and J.H.B. Chenier**, *Ind. Eng. Chem.*, 47, pp 1454-1458, 1955.
19. **Kaplan, S.I. and A.S. Reformatskaya**, *Zh. Obschch. Khim.*, 7, p 545, 1937.
20. **Gillespie, P.C., J.R. Cunningham, and G.M. Wilson**, *Experimental Results from the Design Institute for Physical Property Data I: Phase Equilibria*, 81, 244, p 26, AIChE, DIPPR, New York, NY, 1985.
21. **Ogorodnikov, S.K., *et. al.***, "Liquid-Vapor Equilibrium in the System Ethylene Glycol-Water," *Zhurnal Prikladnoi Khimii*, 35, 3, pp 663-665, March, 1962.
22. **Tombaugh, R.M. and H.S. Chogwill**, "Some Physical Properties of the Ternary System: Ethylene Glycol-Diethylene Glycol-Water," *Transactions of the Kansas Academy of Science*, 54, pp 411-419, 1951.
23. **Trimble, H.M. and W. Potts**, *Ind. Eng. Chem.*, 27, pp 66-68, 1935.
24. *UCC Product Bulletin*, "Glycols," 1971.
25. **Kireev, V.A. and A.A. Popov**, *Zhurnal Prikladnoi Khimii*, Leningrad, 7, p 490, 1934.
26. **Skripach, T.K. and M.I. Temkin**, "Studies of the Equilibrium Liquid-Vapor in the Systems: Water-Ethylene Glycol, Water-Diethylene Glycol, Ethylene Glycol-Diethylene Glycol, Diethylene Glycol-Triethylene Glycol," *Zh. Prikl. Khim.*, 19, pp 180-186, 1946.
27. **Sokolov, N.M., L.N. Tysgankova, and N.M. Zhavoronkov**, *Teor. Osn. Khim. Tekhnol.*, 5, 6, pp 900-904, 1971.
28. **Villamañán, M.A., C. Gonzales, and H.C. Van Ness**, "Excess Thermodynamic Properties for Water/Ethylene Glycol," *J. Chem. Eng. Data*, 29, 4, pp 427-429, 1984.
29. **Herskowitz, M. and M. Gottlieb**, "Vapor-Liquid Equilibrium in Aqueous Solutions of Various Glycols and Poly(ethylene glycols), 2. Tetraethylene Glycol and Estimation of UNIFAC Parameters," *J. Chem. Eng. Data*, 29, 4, pp 450-452, 1984.
30. **Tsuji, T., T. Hiaki, and M. Hongo**, "Vapor-Liquid Equilibria of the Three Binary Systems: Water + Tetraethylene Glycol (TEG), Ethanol + TEG, and 2-Propanol + TEG," *Ind. Eng. Chem. Res.*, 37, 5, pp 1685-1691, 1998.
31. **Liu, H. and Y. Hu**, "Equation of State for Polymer Systems," *Fluid Phase Equilibria*, 150-151, pp 667-677, 1998.
32. **Eliassi, A., H. Modarress, and G.A. Mansoori**, "Measurement of Activity of Water in Aqueous Poly(ethylene glycol) Solutions (Effect of Excess Volume on the Flory-Huggins c-Parameter)," *J. Chem. Eng. Data*, 44, 1, pp 52-55, 1999.
33. **Herskowitz, M. and M. Gottlieb**, "Vapor-Liquid Equilibrium in Aqueous Solutions of Various Glycols and Poly(ethylene glycols), 3. Poly(ethylene glycols)," *J. Chem. Eng. Data*, 30, 2, pp 233-234, 1985.
34. **Virtanen, P.O.I.**, "The Variation of the Rate of Hydrolysis of Ethylene Oxide with the Water Content of the Solvent," *Suomen Kemistilehti*, 38B, 7-8, pp 135–142, 1965.
35. **Leung, J.C. and H.G. Fisher**, "Runaway Reaction Characterization: A Round-Robin Study of Three Additional Systems," *International Symposium on Runaway Reactions, Pressure Relief Design and Effluent Handling*, G.A. Melhem and H.G. Fisher, Editors, pp 109–134, AIChE, DIERS, New York, NY, 1998.
36. **Fisher, H.G., *et. al.***, "Emergency Relief System Design Using DIERS Technology—The DIERS Project Manual," AIChE, DIERS, New York, NY, 1992.
37. *Guidelines for Pressure Relief Design and Effluent Handling Systems*, AIChE, Center for Chemical Process Safety, New York, NY, 1998.